Environmental Pollution 322 (2023) 121237

Contents lists available at ScienceDirect

Environmental Pollution

journal homepage: www.elsevier.com/locate/envpol

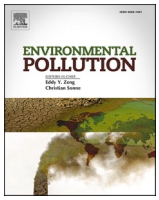

DOM influences Hg methylation in paddy soils across a Hg contamination gradient☆

Mahmoud A. Abdelhafiz [a,b,c], Jiang Liu [a], Tao Jiang [a,d], Qiang Pu [a], Muhammad Wajahat Aslam [a], Kun Zhang [a], Bo Meng [a,*], Xinbin Feng [a]

[a] State Key Laboratory of Environmental Geochemistry, Institute of Geochemistry, Chinese Academy of Sciences, Guiyang, 550081, China
[b] University of Chinese Academy of Sciences, Beijing, 100049, China
[c] Geology Department, Faculty of Science, Al-Azhar University, Assiut, 71524, Egypt
[d] Interdisciplinary Research Centre for Agriculture Green Development in Yangtze River Basin, College of Resources and Environment, Southwest University, Chongqing, 400716, China

ARTICLE INFO

Keywords:
Mercury
Dissolved organic matter
Allochthonous and autochthonous DOM
Rice paddy soil
Hg methylation

ABSTRACT

Rice paddies provide optimum conditions for Hg methylation, and paddy soil is a hot spot for Hg methylation and the predominant source of methylmercury (MeHg) accumulated in rice grains. The role of dissolved organic matter (DOM) in controlling Hg bioavailability and methylation in rice paddy systems remains unclear. Paddy soils from eight various cultivation sites in China were chosen to investigate the variations in soil DOM and the influence of DOM concentration and optical characteristics on Hg methylation in rice paddy systems. In the present study, 151 rhizosphere soil samples were collected, and UV–Vis absorption and fluorescent spectroscopy were used to identify the optical properties of DOM. The relationship between MeHg and DOM's optical property indices revealed the production of MeHg consumes lower molecular weight DOM. Moreover, the correlation between DOM concentration and its optical characteristics highlighted the significant role of humic components on MeHg variability in paddy soil. Variation and correlation results demonstrated the allochthonous origin of DOM in the Hg-contaminated soil, with a higher molecular weight and humic character of DOM, as well as the dominant role of autochthonous DOM in promoting Hg methylation in uncontaminated soil. The current study indicated that soil organic matter and its dissolved fractions tend to limit Hg bioavailability and subsequently diminish MeHg production in contaminated paddy soils. Furthermore, the leading roles of allochthonous DOM in protecting MeHg from degradation and autochthonous DOM signatures in enhancing MeHg production in paddy soils. Overall, these findings provide insight into the correlative distributions of DOM and Hg along a Hg concentration gradient in paddy soil, thereby highlighting their potential role in controlling Hg bioavailability and regulating Hg methylation in the soil ecosystems.

1. Introduction

As one of the serious environmental pollutants, mercury (Hg) and its organic form methylmercury (MeHg) have gained significant attention due to their neurotoxicity to biota. Because of their recurrent wet-dry cycles and abundant substrates for microbial activity, shallow flooded systems (e.g., rice paddies) provide optimum conditions for Hg methylation; therefore, paddy soil was identified as a hotspot of Hg methylation and the predominant source of MeHg accumulated in rice (Hall et al., 2008; Meng et al., 2010, 2011; Zhao et al., 2016a, 2016b). Rice was recognized as a bioaccumulator for MeHg (Gustave et al., 2019; Meng et al., 2011; Qiu et al., 2008); furthermore, MeHg bioaccumulation in rice grains can result in significant MeHg exposure to humans through rice consumption (Feng et al., 2008; Zhang et al., 2010), which can be enriched in the human body due to its ability to cross the blood-brain barrier, posing health risks (Beckers and Rinklebe, 2017).

Organic matter (OM), pH, redox potential (E_H), and microbial activity are known factors influencing the speciation of Hg in natural environments and therefore determine the mobility and bioavailability of

☆ This paper has been recommended for acceptance by Jörg Rinklebe.
* Corresponding author.
E-mail address: mengbo@vip.skleg.cn (B. Meng).

https://doi.org/10.1016/j.envpol.2023.121237
Received 12 December 2022; Received in revised form 5 February 2023; Accepted 6 February 2023
Available online 7 February 2023

Hg (Beckers et al., 2019a, 2019b; Frohne et al., 2012; Liu et al., 2014; Pu et al., 2022; Ullrich et al., 2001; Wang et al., 2021; Yang et al., 2007). In which dissolved organic matter (DOM), a complex and heterogeneous continuum of organic molecules ranging from low to high molecular weight, is the most active component in the soil carbon pool, playing an essential role in environmental soil chemistry (nutrient circulation, the transportation of soil pollutants) and climate change (Chen et al., 2020; Gerbig et al., 2011). As the most mobile OM and an essential constituent pool of the bulk soil organic matter (SOM), DOM in soils can reflect the total SOM and predict its transformations (Kuzyakov et al., 2018). The role of DOM on Hg fate has been extensively studied in different environments. DOM affects Hg redox reactions and complexation, influencing microbial Hg uptake and methylation in sediments, floodplain soils, and water (Beckers et al., 2019a, 2019b; Bravo et al., 2017; Dong et al., 2010; Lin et al., 2014; Wang et al., 2021). Multiple studies reported that higher levels of DOM increased Hg bioavailability, methylation, and bioaccumulation (Frohne et al., 2012; Gerbig et al., 2011; Hsu-Kim et al., 2013; Schartup et al., 2013; Wang et al., 2021), where labile fractions are relatively high and readily biodegradable; it may enhance methylation by stimulating microbial growth (Bravo et al., 2017; French et al., 2014; Graham et al., 2013; Mazrui et al., 2016). Conversely, Barkay et al. (1997), Watras et al. (1998), and Hammerschmidt et al. (2008) showed that DOM inhibits microbial Hg methylation due to Hg bioavailability reduction caused by the formation of strong complexation of Hg with DOM. To bridge this knowledge gap, the DOM's optical properties are supposed to contribute to its explanation which were not fully understood previously, especially in the paddy soil environments. Together with the role of soil DOM characteristics on the bioavailability of Hg in methylation in paddy soil remains unclear to date. Therefore, we conducted this study to find the linkage between soil DOM characteristics and Hg methylation in rice paddies.

UV–Vis and excitation-emission matrices (EEMs) have been applied as potential methods for identifying DOM's structure, composition, and sources in different ecosystems (Bravo et al., 2017; Coble et al., 2014; Eckley et al., 2021; Wang et al., 2022b), which are recognized as powerful tools for elucidating the environmental fates of contaminants (Jiang et al., 2018, 2017; Kim et al., 2017; Lescord et al., 2018). Jiang et al. (2018) used UV–Vis and EEMs to study the influence of DOM characteristics on dissolved Hg species in sediment porewater of three lakes in southwest China and found essential links between specific DOM components and the fate of Hg in the lakes. Wang et al. (2022b) demonstrated the effectiveness of UV–Vis and EEMs in determining DOM properties and components in farmland and forestland. In terms of soil environment, the change of land from native to cultivated alters the quality and quantity of DOM; in addition, seasonal fluctuations frequently result in variations in temperature, precipitation, microbial activity, and other factors that can affect DOM properties (Praise et al., 2020; Tong et al., 2021). Changes in DOM properties can reflect changes in the soil environment. Though, changes in soil DOM characteristics with Hg species, mainly production of net MeHg, in different paddies have been rarely studied.

Despite the link between the concentration of DOM and Hg or/and MeHg in aquatic and terrestrial systems becoming clearer as identified by several reports (Bergamaschi et al., 2012; French et al., 2014; Jiang et al., 2018, 2017; 2020; Lescord et al., 2018; Wang et al., 2022a); understanding how DOM's chemodiversity differed in diverse paddy soil and the influence of DOM properties on Hg bioavailability and methylation in rice paddy systems remains relatively nascent. According to our previous work (Liu et al., 2022a), DOM-Hg had a high Hg methylation rate, even higher than aqueous Hg(II) in paddy soils. Notably, organic matter-bound Hg is the dominant Hg fraction for ambient Hg pool and newly deposited in paddy soils (Liu et al., 2022b). Therefore, more information related to DOM in different paddy fields is needed for a robust understanding of how DOM in paddy soil influences Hg behaviors. We hypothesized that DOM influences not only MeHg production but also affects its accumulation in paddy soils. To verify our hypothesis, paddy soils from eight various cultivation sites in southwestern China, the world's largest rice producer, which accounts for approximately 28% of global rice production (Yuan and Peng, 2022), were selected to figure out (i) variations in DOM and Hg species in diverse rice paddy soil, and (ii) the potential relationships between the concentration/optical properties of DOM and net MeHg production to explore its roles on MeHg accumulation and, consequently, its potential effects on Hg methylation in rice paddy fields across a Hg concentration gradient. The present work is the cornerstone for further explaining DOM's chemical compositions and fractions, and the relation with Hg to explain the fate of Hg in rice paddies.

2. Methodology

2.1. Study area description

Eight paddy fields in China, including contaminated and uncontaminated sites, were chosen for sample collection (Fig. 1 and Fig. S1). As per the numbers, four sites are located in Guizhou province, China; three are situated in Wanshan Hg mining area, which was historically China's largest Hg mine (Feng and Qiu, 2008). Those three sites comprise an artisanal Hg mining site (Gouxi [GX]), and two abandoned Hg mining sites (Sikeng [SK] and Wukeng [WK]) (Zhao et al., 2016a, 2016b). Huaxi (HX), southwest of Guiyang, Guizhou, is a Hg non-polluted site, and no point sources of Hg pollution have been identified. One site in Xunyang (XY) from the antimony-mercury (Sb–Hg) mining area in Shaanxi province was selected as a contaminated site. High Hg contamination was reported in the paddy fields of this region (Ao et al., 2020; Qiu et al., 2011). Three sites from the largest heavy metals smelters, namely Hengyang (HY), Shuikoushan (SKS), and Zhuzhou (ZZ), in Hunan province, were included. The studied locations were chosen as they represent the diversity in mercury levels, from contaminated sites with varied sources of Hg pollution to uncontaminated areas.

2.2. Sample collection and preparation

A total of 151 ($n = 151$) soil samples from the root zone (10–20 cm depth) were collected in this study from GX ($n = 22$), SK ($n = 10$), WK ($n = 10$), HX ($n = 15$), XY ($n = 21$), HY ($n = 25$), SKS ($n = 24$), and ZZ ($n = 24$) during the 2020 harvest season (Fig. S1). At each sampling site, the soil samples were stored in polypropylene tubes (JET®, China) with no headspace and sealed with Parafilm®. Soil samples were brought back to the laboratory in coolers with ice packs (~4 °C) within 24 h and kept at −20 °C before freeze-drying. Freeze-dried (−80 °C; Eyela FDU-2110, China) samples were screened to pick gravels/residues, ground, and mixed homogeneously using a mortar and pestle to pass through 200 mesh. Before each operation, all tools involved in grinding were thoroughly cleaned to avoid cross-contamination. Processed soil samples were stored in polyethylene zip-lock bags at ~4 °C before analysis. All possible measures were considered to prevent cross-contamination during sample collection and preparation.

2.3. Analytical methods

2.3.1. Soil DOM extraction

The DOM in soil was extracted using Milli-Q water with a water to soil ratio (v/w) of 10:1 on a horizontal shaking device (200 r min^{-1}) at room temperature (~22 °C) in dark conditions for 18 h. Then, the suspension was centrifuged at 4000 rpm (RCF of 2850 g) for 30 min (Liu et al., 2021). The supernatant was filtered using 0.45 μm mixed cellulose acetate filters (Whatman, USA). The isolated filtrates were kept in a refrigerator at ~4 °C under dark conditions for further analysis.

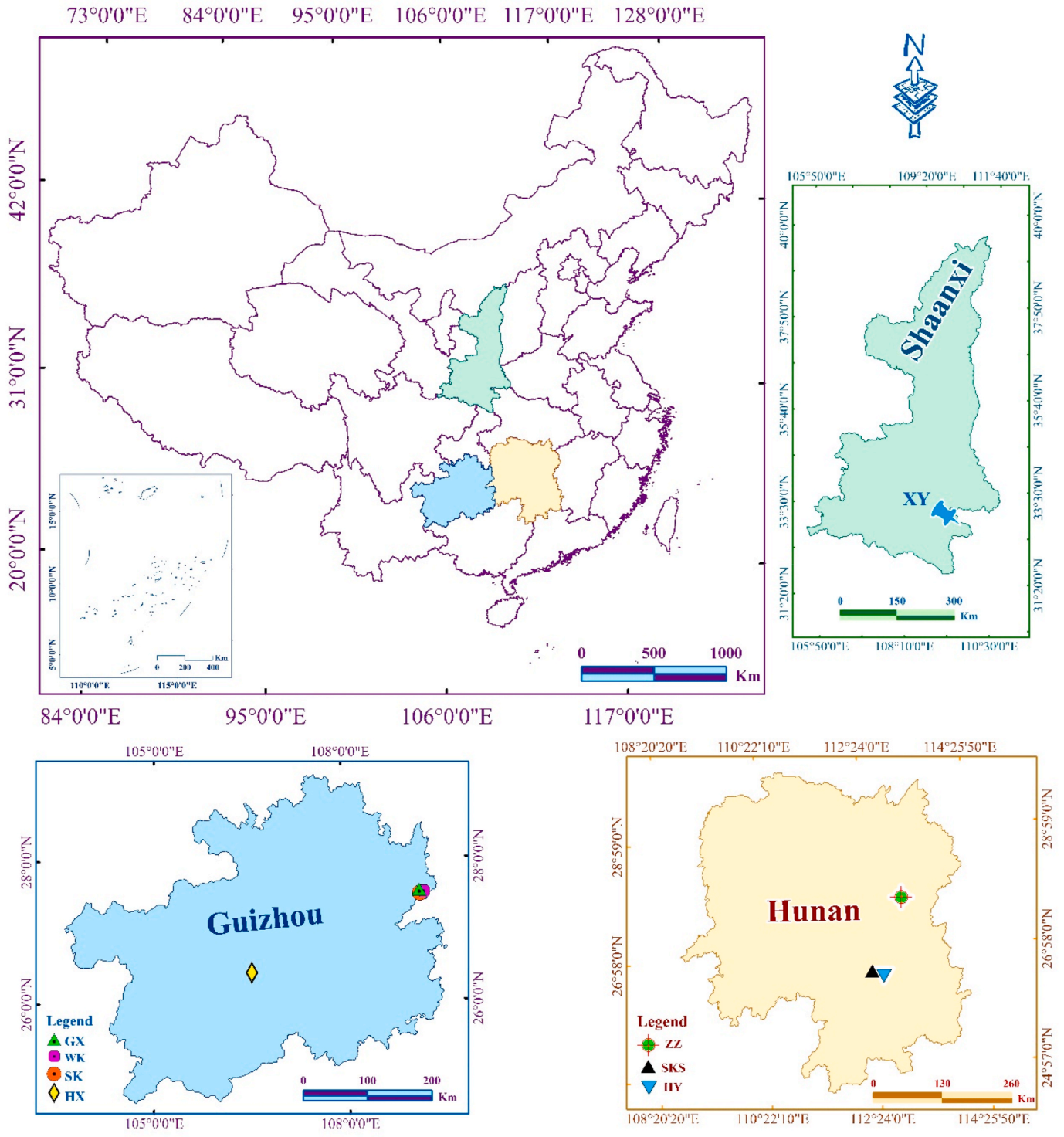

Fig. 1. Geographical map of China with location maps of the collected paddy soils from three provinces of China. Four sites are located in Guizhou province, including GX (Gouxi), WK (Wukeng), SK (Sikeng), and HX (Huaxi). In Hunan province, we selected three locations for sampling, ZZ (Zhuzhou), SKS (Shuikoushan), and HY (Hengyang). One site in Xunyang (XY) from the antimony-mercury (Sb–Hg) mining area in Shaanxi province was selected. Details regarding samples locations are shown in Fig. S1.

2.3.2. *Characterization of DOM and relevant parameters*

The pH values of the soil samples were measured using a pH electrode (SX751 pH/ORP/Cond/DO meter, SANXIN, China) with a soil: water ratio (w/v) of 1:2.5. A total organic carbon analyzer (TOC-V, Shimadzu, Japan) was used to determine soil DOM concentration, expressed as dissolved organic carbon (DOC) in mg g^{-1}. The SOM content of paddy soil was estimated using loss on ignition (LOI) method (Nayak et al., 2019). An Aqualog® absorption–fluorescence spectrometer (Horiba, Japan) was used to acquire UV–Vis and fluorescence measurements. Aqualog® EEMs data processing software automatically corrected EEMs for the inner-filter effect. It modified the instrument-specific excitation and emission effects using parallel absorbance measurements from the same sample and blank (Yang and Hur, 2014). The UV–Vis scan range was from 230 to 800 nm at 1 nm

intervals. Fluorescence spectra were used to record EEMs. The absorption coefficient at 355 nm a (355) represented the abundance of chromophoric DOM (CDOM) (Zhang et al., 2005). The fluorescence index (FI) was commonly employed to identify DOM sources, either allochthonous or autochthonous and/or a combination of both, as the ratio of fluorescence intensities at 450 and 500 nm E_m wavelengths (E_x wavelength was kept at 370 nm). Allochthonous and autochthonous sources were differentiated by FI values below 1.4 and above 1.9, respectively (Huguet et al., 2009). As an indicator for reflecting the DOM's humic content or humification degree, the humification index (HIX) was calculated as the ratio of fluorescence over E_m 255/434-480 nm to that over 255/300–346 nm (E_x/E_m) (Ohno, 2002). Details regarding the characteristics of DOM, including absorption coefficient calculation, specific UV absorbance, the fluorescence compounds and indices, are described in the supplementary information (Text S1 and Table S1).

2.3.3. Mercury analysis

THg quantification was done using cold vapor atomic fluorescence spectrophotometer (CVAFS) system (Brooks Rand Model III, Brooks Rand Laboratories, USA). Approximately 0.1–0.25 g soil sample was weighed and digested in the glass tube by adding 5 mL of a fresh mixture of aqua regia ($HCl:HNO_3 = 3:1$ v/v) at 95 °C in a water bath for 55 min. 0.5 mL of bromine chloride oxidation (BrCl, 25%) was added 10 min from the digestion started. Following digestion, the samples were cooled and diluted with distilled deionized water (DDW, Milli-Q®, Millipore, USA) to a final volume of 25 mL. After 24 h, the supernatant was collected, and THg was determined using CVAFS, which was preceded by $SnCl_2$ reduction, purging with N_2, and gold trap amalgamation (USEPA, 2002). A 0.25–0.40 g soil sample was prepared according to the $CuSO_4^-$ methanol/solvent extraction method to analyze MeHg. CVAFS was used to detect MeHg in samples after N_2 purging, Gas chromatography (GC) separation, and thermal decomposition to Hg^0 steps following the USEPA method 1630 (Liang et al., 1996; USEPA, 2001, 2017). Analytical-grade chemical reagents were used in all experiments; moreover, the ultra-cleaning ensured extremely low Hg blanks. The detailed procedure is explained in Text S2.

2.4. QA/QC and statistics

Calibration curves with the coefficient of variation ($r^2 \geq 0.999$) were obtained for all batches analyzed for THg and MeHg. For each batch of samples, every tenth sample was triplicated, along with certified reference materials, and method blanks were employed. Except for the original sample, method blanks contained all reagents used to digest various THg and MeHg analysis samples using the given methods. Method detection limits (3σ) for soil samples were recorded as 0.01 ng g^{-1} (THg) and 0.002 ng g^{-1} (MeHg). Relative standard deviation (RSD %) for triplicates was less than 6.1% and 4.4% for THg and MeHg, respectively. Certified reference materials employed in this study and the recoveries are given in Text S3. All measured parameters were statistically analyzed using SPSS software (Version 28, IBM® Inc. IL, USA) and expressed as mean ± SD. A random forest model (*RF*-M) was performed using the "randomForest" package and R software. For correlation analysis, Pearson's r and Spearman's r were employed; the former was used for normally distributed datasets, while the latter was performed for non-normal distributed data. A statistically significant difference was set at $p < 0.05$ and $p < 0.01$. A nonparametric statistical model with Kolmogorov–Smirnov (*K–S*) test was performed to identify the differences between diverse independent datasets used in our research. Further details of the statistical analysis are given in Text S3.

3. Results

3.1. SOM and DOM quantity

Soil organic matter (SOM), pH, as well as soil DOM concentrations and optical properties in the studied samples from various sites are shown in Fig. S2. The average (range) SOM% of paddy soil in each location is 10.36 ± 1.11 (8.26–13.40), 6.80 ± 1.16 (4.92–9.23), 5.18 ± 0.55 (4.09–5.97), 6.39 ± 0.65 (4.97–7.08), 6.21 ± 1.02 (5.16–9.58), 6.05 ± 1.07 (3.01–7.43), 6.00 ± 0.99 (3.72–7.68), and 7.70 ± 1.57 (5.33–10.44) at HX, GX, SK, WK, HY, SKS, XY, and ZZ, respectively (Table S2). Significant differences between HX, ZZ, and SK (one-way ANOVA $p < 0.05$) were observed; however, there were no discernible differences in the content of SOM among the other studied sites (Fig. S2a). Higher soil pH values were observed at HX, XY, SK, and GX than at other sites ($p < 0.05$) (Fig. S2b). Among all sites, the highest DOC was found at HX (0.64 ± 0.20 mg g^{-1}) and followed by WK 0.52 ± 0.22 (0.19–0.86) mg g^{-1}, GX 0.40 ± 0.14 (0.24–0.73) mg g^{-1}, ZZ 0.27 ± 0.09 (0.16–0.45) mg g^{-1}, HY 0.27 ± 0.09 (0.15–0.44) mg g^{-1}, XY 0.27 ± 0.05 (0.16–0.34) mg g^{-1}, SK 0.26 ± 0.09 (0.19–0.44) mg g^{-1}, and SKS 0.23 ± 0.09 (0.09–0.41) mg g^{-1} (Fig. S2c and Table S2).

3.2. DOM characteristics

3.2.1. UV–vis absorption characteristics of DOM

The chromophoric DOM (CDOM) indicated by a (355) ranged from 0.14 to 10.95 m^{-1}. The average CDOM values in soil samples were the highest at HY (3.88 ± 3.16) and the lowest (1.53 ± 1.04) at XY (one-way ANOVA $p < 0.05$, Fig. S2d). Regarding mean CDOM contents, the studied sites were in the order of HY > HX > WK > GX > SK > ZZ > SKS > XY (Fig. S3). Specific UV absorbance at the selected λ nm was computed after Fe background absorbance was corrected by dividing the absorbance at λ nm with the corresponding DOC content. No distinct difference in the UV–vis absorbance at 260 and 280 nm was observed; in addition, due to conjugated rings' absorbance at 254 nm (Weishaar et al., 2003), we selected specific UV absorbance at 254 and 260 nm ($SUVA_{245}$ and $SUVA_{260}$) to estimate DOM's hydrophobic structures and aromaticity. As $SUVA_{245}$ and $SUVA_{260}$ exhibited the same trend in the studied samples (Fig. S4b), $SUVA_{245}$ was used as an indicator of DOM aromaticity in our study. The values of $S_{275\text{-}295}$ in paddy soil ranged from 0.010 to 0.025 (nm^{-1}) (Table S2). $S_{275\text{-}295}$ showed a similar pattern as spectral slope compatible with $SUVA_{254}$, particularly at SKS, with the highest (1.55 ± 0.45) and lowest (0.013 ± 0.003) mean values of $SUVA_{254}$ and $S_{275\text{-}295}$, respectively (one-way ANOVA $p < 0.05$, Table S2). Further detailed $SUVA_{254}$, spectral slope (S_R), and $S_{275\text{-}295}$ results are shown in the supplementary information (Text S4).

3.2.2. Fluorescence characteristics of DOM

The fluorescence spectra revealed four fluorescent peaks in paddy soil samples. Peaks A and C indicate humic-like components, whereas protein-like components are represented by peaks B and T. The average levels of humic-like components (peaks A and C) in the studied locations exhibited the highest at HX, followed by WK and HY, and were significantly low at SKS and ZZ (one-way ANOVA, $p < 0.05$, Figs. S2g, S2h, and S5). The higher protein peak signatures, notably peak B, were detected in SKS, HY, and XY paddy soils (one-way ANOVA, $p < 0.05$, Figs. S2i and j). DOM in rice paddies can be characterized using the FI, HIX, and biological index (BIX). FI values for paddy soil samples were between 1.4 and 1.9, revealing a joint autochthonous and allochthonous contribution to DOM (Huguet et al., 2009; McKnight et al., 2001), with one sample of XY and ZZ showing FI values slightly lower than 1.4 and higher than 1.9, respectively (Figs. S6 and S7).

The primary trend of FI in the studied locations was significantly low in Hg mining areas (GX, SK, and WK) and XY (one-way ANOVA, $p < 0.05$, Fig. S7a and Table S3). BIX is a useful indicator of autochthonous inputs and recent microbially-produced DOM. As shown in Fig. S6, BIX

values were below 0.8 for paddy soil samples collected from all locations, confirming the contribution of both allochthonous and autochthonous sources as observed in the previous study (Wang et al., 2022b). HIX results in the studied locations were much less than 10, implying low humification content in rice paddies. SKS recorded the lowest HIX levels with the mean value 0.09 ± 0.05 with significant differences between other paddies (one-way ANOVA, $p < 0.05$). The BIX and HIX values were significantly the highest and the lowest at HY and SKS ($p < 0.05$, Figs. S7b and S2k and Table S3), respectively, further verifying less humification and the more contribution of biologically-derived autochthonous DOM in HY soil that agrees with protein-like components results.

3.3. Mercury species in paddy soil

As shown in Fig. 2a and Table S4, the average (range) THg concentration increased from 0.25 ± 0.14 (0.05–0.62) mg kg^{-1} at SKS to 0.32 ± 0.15 (0.17–0.64), 0.45 ± 0.37 (0.17–1.51), 0.49 ± 0.07 (0.38–0.71), 12.7 ± 11.9 (0.39–76.5), 14.1 ± 13.9 (0.6–47.8), 26.2 ± 47.2 (1.1–155), and 380 ± 333 (22–979) mg kg^{-1} at HX, HY, ZZ, XY, GX, WK, and SK, respectively. It is noted that the range of THg at site SK is irregularly large (22–979 mg kg^{-1}). Spatial variations of methylmercury (MeHg) among eight locations in rhizosphere paddy soils are shown in Fig. 2b. The measured averages of MeHg at HX, GX, SK, WK, HY, SKS, XY, and ZZ were 1.24 ± 0.52, 2.42 ± 1.6, 3.11 ± 1.5, 1.16 ± 0.62, 0.52 ± 0.48, 0.38 ± 0.25, 2.01 ± 1.34, and 0.60 ± 0.32 μg kg^{-1}, respectively (Table S4). The lowest MeHg was recorded at SKS, followed by HY, ZZ, WK, HX, XY, GX, and the significantly highest at SK ($p < 0.05$, Fig. 2b). Though MeHg showed the same trend as THg, the concentrations in paddy soil from the antimony Hg mining site (XY) were significantly higher than in the WK Hg mining area.

Net Hg methylation potential (% MeHg) was estimated in this study as [MeHg]/THg] ratios (%) (Liu et al., 2020). The highest and lowest MeHg/THg ratios were observed at HX (0.004%) and SK (0.00003%), respectively (one-way ANOVA $p < 0.05$, Fig. 2c and Table S4). %MeHg, a valuable factor and relevant proxy for the net Hg methylation potential (Drott et al., 2008; Paranjape and Hall, 2017), is primarily controlled by THg levels. It cannot be used as an indicator showing Hg methylation efficiency from the overall data set due to the wide ranges of THg contents, particularly in Hg-contaminated fields. To apply %MeHg in this study and to clearly discuss and understand the DOM behavior with Hg methylation in rice paddy soil, we divided the eight sites into two groups as per Hg concentrations. Notably, we integrated data from HX, HY, SKS, and ZZ ($n = 88$) as an uncontaminated group since THg levels in the Hg mining area (GX, WK, and SK) and Sb–Hg mining site (XY) ranged between 2 and 3 orders of magnitude higher than that in those locations. Therefore, the contaminated group encompasses SK, WK, GX, and XY ($n = 63$) fields.

4. Discussion

4.1. Overview of DOM and Hg in paddy soil

Correlations between Hg species and DOM concentration and composition were applied using the whole data set of this study to show interactions of DOM with Hg in paddy soils (Table S5). The relations between THg with soil DOC and MeHg with SOM were not detected in the current results (Table S5). The methylation of Hg in the environment cannot be explained solely by OM concentration (Frohne et al., 2012; Schartup et al., 2013). Thus, the optical measures of DOM characteristics are hypothesized to be a valuable tool and a more critical factor influencing Hg species, particularly Hg methylation, in rice paddy soils than total DOM alone. Previous studies in aquatic environments, including sediment porewaters, floodplain soils, and wetlands, reported significant correlations between DOC and THg or MeHg (Beckers et al., 2019a, 2019b; Bergamaschi et al., 2012; Dittman et al., 2009; Frohne et al., 2012; Jiang et al., 2018; Wang et al., 2021). Here, we found a positive correlation between DOC and MeHg in the collected paddy soils ($r =$

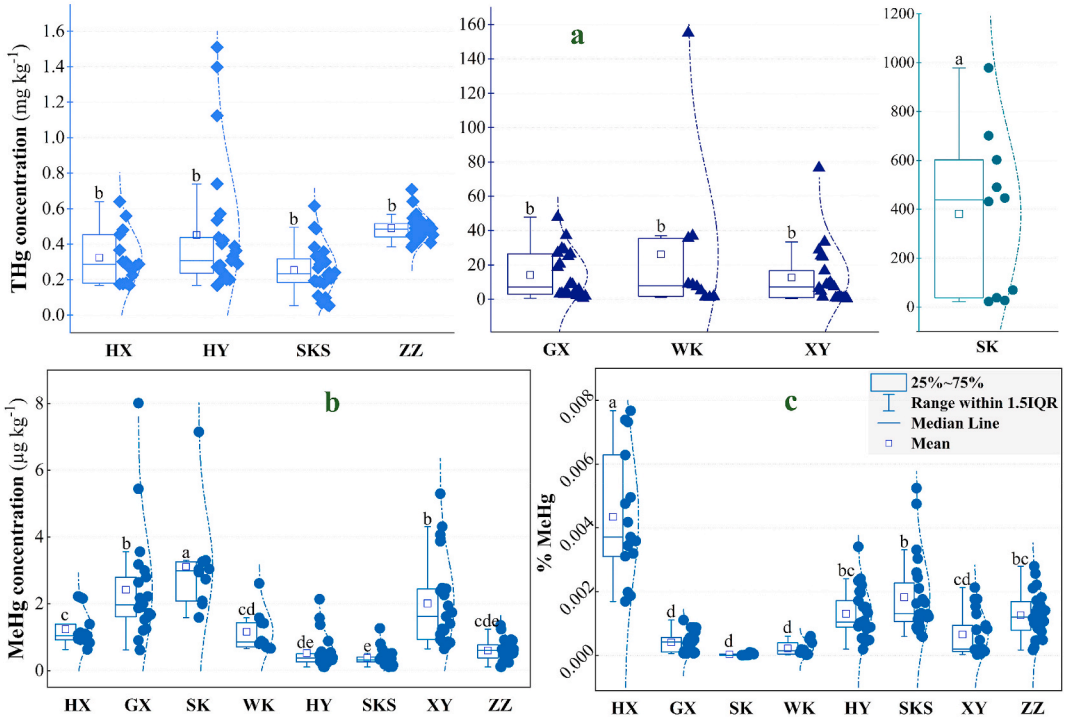

Fig. 2. THg (a), MeHg (b), and % MeHg (c) box plots in different locations of paddy soil. The boxes show the 25th quartile and 75th quartile. Squares and horizontal blue lines in the boxes represent mean and median values. Different lowercase letters on the box plots indicate that the differences in each optical index of DOM are significant through one-way ANOVA with Duncan's post-hoc test ($p < 0.05$). (For interpretation of the references to colour in this figure legend, the reader is referred to the Web version of this article.)

0.25, $p < 0.01$) (Table S5). It suggests that the most mobilizable or labile SOC fraction co-varied with MeHg. In addition, MeHg positively correlated with humic-like fluorescence peak A ($r = 0.22$, $p < 0.01$) and peak C ($r = 0.24$, $p < 0.01$), nonetheless negatively associated with protein-like fluorescence peaks B ($r = -0.46$, $p < 0.01$) and T ($r = -0.36$, $p < 0.01$), which may imply either (i) the humic-like substances or compounds in DOC could bind with MeHg; or (ii) the production of MeHg consumes lower molecular weight DOC (e.g., protein-like substances) (Lee et al., 2018; Liu et al., 2021; Luo et al., 2022).

Regarding the former, humic substances could bind with MeHg and inhibit it from degradation, together with protein-like peaks B and T could be the biodegradation products of peaks A and C, suggesting the biodegradation of humic substances occurred with MeHg degradation simultaneously (Amirbahman et al., 2002; Hintelmann et al., 1995; Luo et al., 2022; Wang et al., 2015). This is supported by the significant positive correlation between MeHg and HIX ($r = 0.56$, $p < 0.01$) and the significant inverse correlations between MeHg and BIX ($r = -0.26$, $p < 0.01$) and FI ($r = -0.42$, $p < 0.01$) (Table S5). Besides, the interaction between DOC and the optical properties of DOM reflected the significant role of humic components on MeHg variability in paddy soil, as denoted by the significant positive association of DOC with HIX ($r = 0.46$, $p < 0.01$), and humic-like peaks A ($r = 0.36$, $p < 0.01$) and T ($r = 0.40$, $p < 0.01$) (Table S5). In terms of the latter, previous studies found that the biodegradation of DOM depleted the lower molecular weight fractions and further humified the original DOM (Lee et al., 2018; Liu et al., 2021). Moreover, the liable DOM could be degraded easily with the presence of microorganisms, whereas some highly humified DOM is too stable to be involved in microbial metabolisms (Lee et al., 2018). Meanwhile, the degradation of labile DOM stimulates Hg methylation (Bravo et al., 2017; Graham et al., 2013), resulting in lower peaks B and T with higher MeHg, as observed in our study. Lescord et al. (2018) reported that the availability of labile DOM could be responsible for the increased Hg bioaccumulation, possibly due to enhanced Hg methylation.

4.2. DOM and Hg variations in contaminated and uncontaminated paddy soils

The difference in DOM (reflected by DOC in mg g^{-1}) content between contaminated and uncontaminated rice paddy soils was significant ($p = 0.048$, Fig. 3). This result aligned with the prior studies, which highlighted that DOM concentration varied significantly among paddy soils in China due to different soil types (Gao et al., 2017; Qin et al., 2020). The DOM concentration differences from our study suggest DOM may influence the fate of Hg in different ways, as when DOM levels are low, it can act as a rate-limiting step in methylation. The optical properties reflect the compositional and structural information of DOM, which shows the chemodiversity of DOM. In this study, the optical properties of DOM varied considerably between contaminated and uncontaminated paddy soils (Fig. 3). Significantly higher S_R was observed at the uncontaminated sites than those at the contaminated sites ($p < 0.001$), suggesting the relatively high molecular weight of DOM in the contaminated paddy soils of this study (Fichot and Benner, 2012; Fichot et al., 2013). The spectral slope is often inversely correlated to the DOM molecular weight (Helms et al., 2008; Jiang et al., 2018, 2020; Spencer et al., 2012). Moreover, significant differences among contaminated and uncontaminated paddy soils were observed after normalizing humic-like substances (peaks A and C) and protein-like substances (peaks B and T) by DOC to avoid concentration dependence. HIX and humic-like fluorescence Peak A/DOC and peak C/DOC were significantly higher in contaminated soil than in uncontaminated ($p < 0.01$, Fig. 3 and Fig. S8), demonstrating paddy soil DOM's humic character in contaminated fields, which agrees with the S_R (Birdwell and Engel, 2010; Jiang et al., 2017). Humic Substance variations between polluted and uncontaminated areas could be related to the effect of pH, which is very sensitive to pH fluctuations (Groeneveld et al., 2022).

Even though the contribution of allochthonous and autochthonous sources reflected by FI results in the studied locations (Fig. S6), FI, BIX, and protein-like signature peaks B/DOC and T/DOC were significantly higher in uncontaminated paddy soil ($p < 0.001$; Fig. 3 and Fig. S8). It suggested that DOM was enrichment by more autochthonous (i.e.,

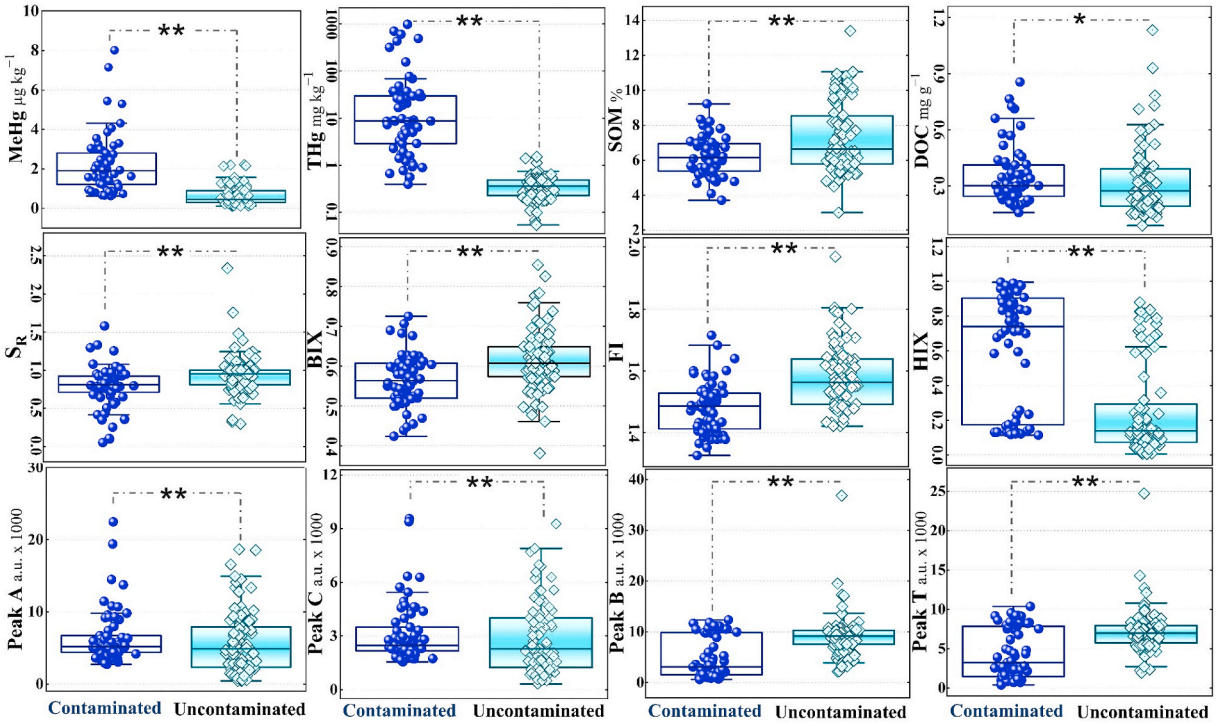

Fig. 3. Box plots showing the significant DOM and Hg variations in contaminated and uncontaminated paddy soils. The boxes show the 25th quartile and 75th quartile. Independent-Samples Kolmogorov-Smirnov Test was used. ** and * indicate that the indices distribution is significant at $p < 0.01$ and $p < 0.05$, respectively.

microbial) than allochthonous (i.e., terrestrial) sources at uncontaminated sites, as the protein-like components are significantly related to microbial activities (Mostofa et al., 2013; Nowicki et al., 2019). The overall BIX and FI contents in the present study were within the previously reported limits for soil DOM, implying that DOM was more influenced by allochthonous than autochthonous sources from different soil types, with more protein-like components from paddy soil (Gao et al., 2017; Qin et al., 2020; Shang et al., 2018).

In terms of Hg species, THg levels decreased in rice paddy soil from contaminated to uncontaminated sites, with an average (range) content of 71.7 ± 183 0.39–979) and 0.39 ± 0.24 (0.05–1.51) mg kg^{-1}, respectively (Fig. 3 and Table S6). MeHg presented the same signature as THg, which was evidently much higher at contaminated sites than in uncontaminated rice paddy soil ($p < 0.001$) (Fig. 3 and Table S6). Du et al. (2021) showed the 30.60 mg kg^{-1} and 14.56 μg kg^{-1} concentrations of THg and MeHg in soil from a typical mining area in China. The current results are consistent with a recent study by Pu et al. (2022). They reported 0.27 mg kg^{-1} as a mean concentration of THg in uncontaminated paddy soil, ranging from 22.15 to 588 mg kg^{-1} in Hg-contaminated areas, showing that Hg concentrations in contaminated soil were three orders of magnitude higher than those at the uncontaminated sites.

4.3. Influences of DOM characteristics on net MeHg concentration in paddy soils along a Hg concentration gradient

Spearman correlation and various models were conducted to explore the influences and contributions of DOM optical properties to Hg methylation in diverse paddy soils. DOC is positively correlated with SOM ($r = 0.49$, $p < 0.01$) and CDOM ($r = 0.33$, $p < 0.01$) (Fig. 4 and Table S7), reflecting the DOM was mainly composited by fractions with a higher molecular weight. This finding is further confirmed by the higher humic components of DOM (i.e., higher HIX, humic-like peak A, and peak C) (Fig. 3) in Hg-contaminated paddy soils. Particularly, MeHg in the contaminated paddy soil is negatively correlated with SOM (Spearman's $r = -0.29$, $p < 0.01$) and DOC (Spearman's $r = -0.33$, $p < 0.01$), suggesting soil organic matters and its dissolved fractions (i.e., DOM) may diminish the bioavailability of inorganic Hg(II) and therefore reduce the production of MeHg potentially. Thus, the Hg contents in highly Hg-contaminated paddy soil are likely influenced by DOM molecular mass distribution, as evidenced by the relationships between MeHg and S_R ($r = -0.32$, $p < 0.05$; Fig. 4). With higher molecular weight and pH, OM has a pivotal role in immobilizing Hg(II), reducing its bioavailability for microbial uptake and consequently inhibiting methylation (Li et al., 2018; Ravichandran, 2004; Zhang et al., 2022). Where the higher pH indicates less mobile Hg fractions and more recalcitrant DOM in paddy soils (Li et al., 2018); moreover, humic compounds would bind with MeHg and protect it from degradation, further supporting our finding reflected by the significant positive correlation between MeHg and humic-like components (in section 4.1). Greater humic compounds in Hg-contaminated areas reported in the former section confirmed this finding. Furthermore, low autochthonous DOM signals (BIX, protein-like peaks B and T) at the contaminated sites (Fig. 3) imply a low microbial activity in contaminated areas, which may decrease MeHg production. Previous studies reported that highly microbially dominant OM components could exhibit elevated microbial activity and production of MeHg (Jiang et al., 2018; Ortega et al., 2018). Another study from our group also reported that Hg stress significantly influences microbial community assembly processes and decreases the ecosystem's multifunctionality (Pu et al., 2022).

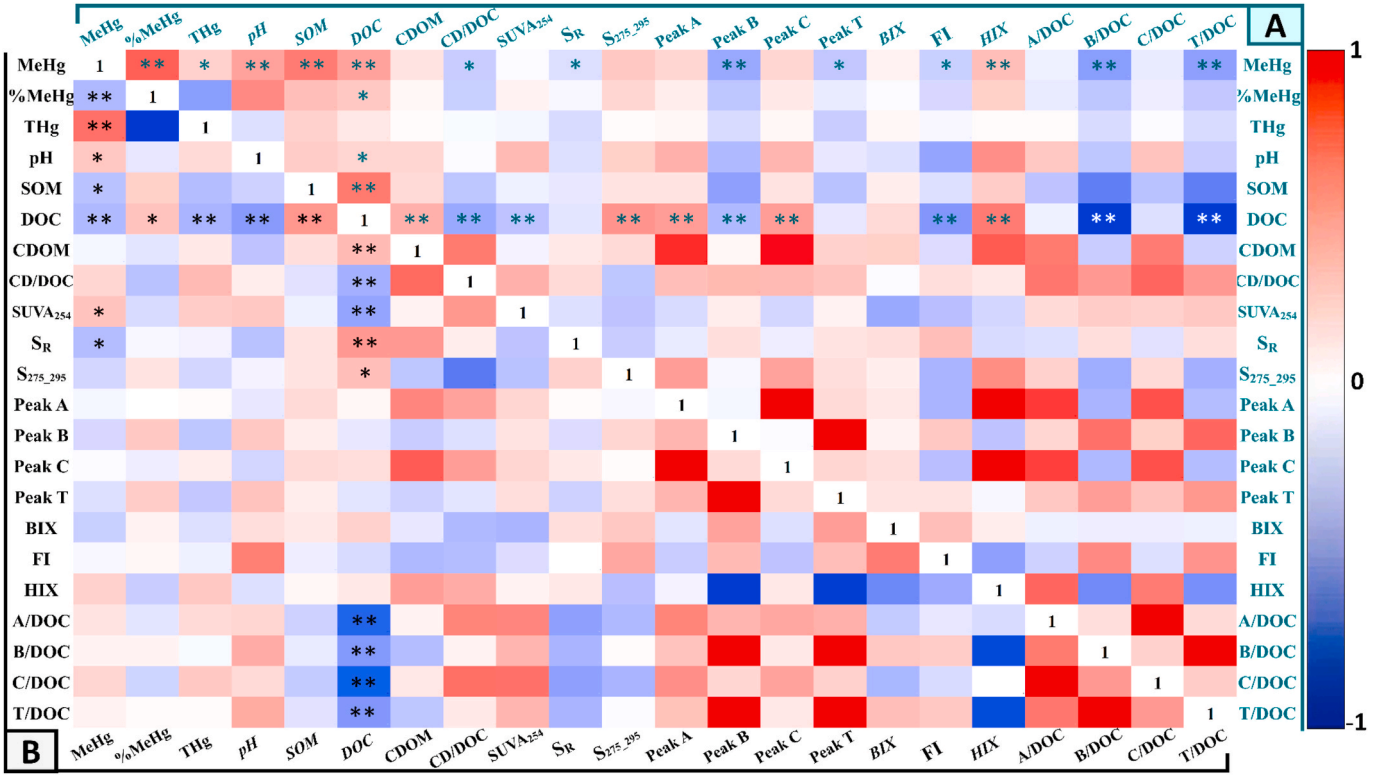

Fig. 4. Heat map showing Spearman's correlation between Hg species, pH, SOM, and DOM concentration and optical characteristics in uncontaminated (A) and contaminated (B) paddy soils. Only significant correlations of MeHg and DOC with other parameters were highlighted (The whole correlation matrix is shown in Tables S5 and S6). * and ** indicate that the bivariate correlations are significant at $p < 0.05$ and $p < 0.01$. Cells with dark colours represent a strong correlation, while light-colored cells reflect weak correlations. CD/DOC is CDOM/DOC, A/DOC and C/DOC = Normalizing humic-like peak A and peak C by DOC; and B/DOC and T/DOC = Normalizing protein-like peak B and peak T by DOC. (For interpretation of the references to colour in this figure legend, the reader is referred to the Web version of this article.)

On the other hand, MeHg strongly positively correlated with SOM ($r = 0.60$, $p < 0.01$) and DOC ($r = 0.44$, $p < 0.01$) at uncontaminated sites (Fig. 4a and Table S8), suggesting that SOM and/or DOM fuels Hg methylation. In uncontaminated paddy soil, MeHg contents were mainly associated with microbial activities (Jiang et al., 2018), as indicated by higher biological signal (BIX), S_R, and FI than in Hg-contaminated soils (Fig. 3). Therefore, we speculate that labile DOM in uncontaminated soils, which is easily degraded, is of prominent importance in MeHg production as it has a pivotal role as a carbon source for Hg methylators (Graham et al., 2013; Lambertsson and Nilsson, 2006; Ortega et al., 2018; Ullrich et al., 2001). According to Frohne et al. (2012), increasing DOC levels in floodplain soils could enhance Hg methylation. Elevated protein-like signature peak B and peak T at uncontaminated sites ($p < 0.001$; Fig. 3) further support the previous explanation that the degradation of DOM associated with microbial activity promotes Hg methylation. As pH was significantly lower at uncontaminated sites than at contaminated sites ($p < 0.001$; Fig. S8), MeHg positively correlated with DOC, and the correlation coefficients of MeHg and peaks B and T are higher than those at contaminated sites. This implies that DOC-regulated Hg methylation depends on the mobility of Hg. Several studies reported enhanced Hg mobility and methylation at low pH (Boening, 2000; Ullrich et al., 2001; Wu et al., 2011). In contrast to contaminated groups, DOC positively correlates to pH and net MeHg production, reflecting paddy soil DOM's vulnerability to degradation. Li et al. (2018) highlighted the vulnerability of DOM to degradation with lower pH in paddy soil. Notably, DOC is negatively correlated with $SUVA_{254}$ ($r = -0.28$, $p < 0.01$), reflecting the role of DOM fraction with lower aromaticity should be highlighted in uncontaminated paddy soil.

Random forest modelling (*RF*-M) was used to identify the most important determinants of DOM's optical data and concentration with net MeHg concentration in rice paddy soil. Furthermore, automatic linear modelling with the forward stepwise method (*FS*-M) was conducted to predict the contributions of DOM optical characteristics to the concentration of MeHg in paddy soils. The *RF*-Model reflected the significant role of OM fraction, which might be more labile, on MeHg variability in paddy soil from the overall data. It is indicated by protein-like substances (peak B/DOC and peak T/DOC) and DOC, which were the primary factors in *RF*-M (Fig. 5A). As MeHg was linked with DOC rather than SOM (Fig. 4), *FS*-M further supports the role of dissolved organic fractions on Hg methylation, as DOC was the most important predictor in paddy soil than SOM (Fig. 5B). The role of humic components in DOC (HIX; Fig. 5A) that can bind with MeHg in paddy soil, as demonstrated by the *RF*-Model, protects it from microbial degradation. In contaminated soils, S_R was the predominant predictor (importance more than 0.3), followed by THg, CDOM, and SOM (Fig. 5B). Furthermore, THg, S_R, and DOC were the critical factors according to random forest modelling (Fig. 5A). CDOM is an important predictor reflected by the *FS* model (Fig. 5B), further supporting the role of allochthonous DOM, which could reduce the availability of Hg for methylation in Hg-contaminated soils (Fig. 4).

Both models emphasized the humic character of the DOM and further confirmed that DOM primarily composited the DOM in Hg-contaminated soil with greater molecular weight. As donated by RF-M, SOM and DOC were the main factors in uncontaminated paddy soil, confirming our finding that OM and its labile fractions could fuel Hg methylation at these sites. Soil pH was the dominant predictor and the highest significant factor ($p < 0.01$) among all the predictors and factors (Fig. 5), reflecting the role of pH in rhizosphere soil, which influences DOM properties (Groeneveld et al., 2022). Moreover, it further demonstrates the role of labile DOM, which is elevated in lower pH (Li et al., 2018), in promoting Hg methylation in uncontaminated soils. The applied models emphasized the significance of DOM aromaticity in the uncontaminated fields, which is consistent with the correlation results. One reason could be that SKS (an uncontaminated paddy field) has the highest DOM aromaticity among all other sites (Fig. S2e), which might be attributed to anthropogenic activities, such as the application of organic wastes, which increase the aromatic degree of soil DOM or naturally, i. g., temperature degrees, which reduce soil DOM aromaticity as temperature rises (Hu et al., 2018; Li et al., 2017).

The random forest model exhibited the effect of protein-like peaks B/

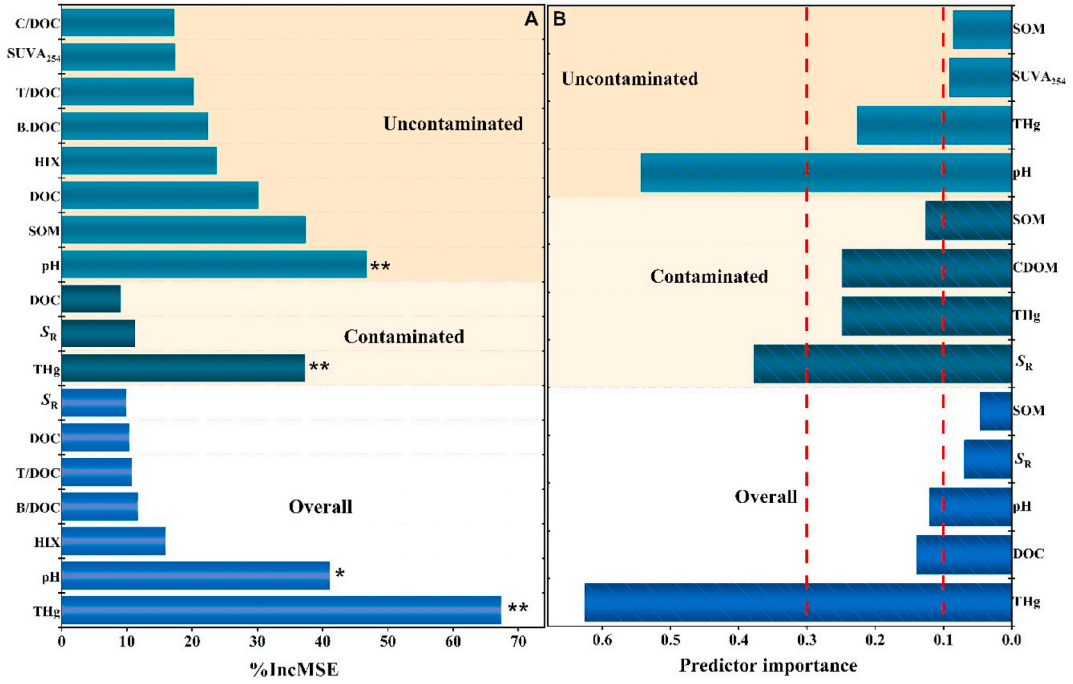

Fig. 5. Random Forest (A) and linear forward stepwise (B) modelling reveal the significance of various factors and predictors for DOM behavior with MeHg in paddy soil. The importance of these factors was estimated using %IncMSE. * and ** indicate the significant different at $p < 0.05$ and $p < 0.01$. In (B), the red dashed lines represent the cutoffs for minor predictors (less than 0.1), important predictors (between 0.1 and 0.3), and highly important predictors (more than 0.3). (For interpretation of the references to colour in this figure legend, the reader is referred to the Web version of this article.)

DOC and T/DOC indices on MeHg, showing the significant contribution of autochthonous inputs in uncontaminated paddy soil. Along with autochthonous DOM, allochthonous sources could be another contributor, as denoted by the HIX factor in *RF*-Model. Humic-like peaks A and C, and HIX significantly positively correlated with DOC ($r = 0.47$, $p < 0.01$) and ($r = 0.47$, $p < 0.01$), and ($r = 0.59$, $p < 0.01$), respectively. It indicates a relative contribution of allochthonous sources to the DOM pool, as noticed by a significantly negative correlation between FI and DOC (Spearman's $r = -049$, $p < 0.01$) in the uncontaminated group. It further demonstrates the role of both autochthonous (i.e., microbial) DOM and allochthonous (i.e., terrestrial) DOM to MeHg in paddy soil, showed by FI results (Fig. S6). In general, Huang et al. (2022), Wang et al. (2022b), and Zhang et al. (2022) highlighted the effectiveness of optical DOM characteristics, which could provide a clue to explain the Hg methylation in soil and heavy metals behaviors in soil and sediments. Our study illustrated that the optical DOM properties showed a good correlation with Hg species in paddy soil, reflecting the usefulness of optical analysis in tracking Hg methylation in this system. Further solid evidence is needed to depict the precise scenario of soil DOM effect on Hg methylation and demethylation in paddy soils.

5. Conclusion

The present study improved our understanding of the crucial role of DOM properties on Hg methylation in rice paddy soil. In summary, the optical measures of DOM properties were found to be more critical factors affecting Hg methylation rates in rice paddy soils than the total DOM. Joint allochthonous and autochthonous DOM inputs were predominant in paddy soil with a more allochthonous effect on MeHg and DOM pool at Hg-contaminated sites. The current study revealed that more signals of autochthonous DOM (BIX, protein-like peak B and peak T) and its correlation with MeHg, implying an enrichment in low molecular weight DOM and a greater autochthonous contribution to Hg methylation in uncontaminated soil. Correlation and statistical model results highlighted the vital role of net MeHg potential in Hg methylation, and DOM, especially protein-like compounds in DOM, promotes Hg methylation in uncontaminated rhizosphere soils. The finding of this study presented an insight into the DOM behaviors in paddies and implied the significant correlations of its characteristics with MeHg in various paddy soil. More efforts are required to uncover the effect of DOM compositions in controlling Hg species and bioavailability across Hg gradient in rice fields. Moreover, continuing work with a novel approach is recommended to clarify soil DOM fractionations that could track Hg fate, particularly the methylation rates, as the rice paddies provide ideal conditions for Hg methylation.

Author statement

Mahmoud A. Abdelhafiz: Data curation; Formal analysis; Investigation; Visualization; Writing - original draft. **Jiang Liu**: Data curation; Investigation; Writing - review & editing. **Tao Jiang**: Formal analysis; Writing - review & editing. **Qiang Pu**: Data curation; Investigation. **Kun Zhang**: Investigation; Formal analysis. **Muhammad Wajahat Aslam**: Formal analysis. **Bo Meng**: Conceptualization; Funding acquisition; Investigation; Methodology; Project administration; Supervision; Validation; Writing - review & editing. **Xinbin Feng**: Conceptualization; Funding acquisition; Project administration; Supervision; Writing - review & editing.

Declaration of competing interest

The authors declare that they have no known competing financial interests or personal relationships that could have appeared to influence the work reported in this paper.

Data availability

Data will be made available on request.

Acknowledgment

This research was funded by the National Natural Science Foundation of China (41931297, 42022024, and 41921004), CAS "Light of West China" program, and the State Key Laboratory of Environmental Geochemistry (SKLEG2021201). Mahmoud Abdelkarim Abdelhafiz Abdallah was supported by the CAS-TWAS president doctoral fellowship program for this research work. The authors are grateful to Ms. Siqi Zhang, Mr. Sihua Zhu, and Ms. Meng Xia from southwest University for helping in analysing the soil dissolved organic matter properties. Finally, we would like to thank the editor and anonymous reviewers for their constructive comments.

Appendix A. Supplementary data

Supplementary data to this article can be found online at https://doi.org/10.1016/j.envpol.2023.121237.

References

Amirbahman, A., Reid, A.L., Haines, T.A., Kahl, J.S., Arnold, C., 2002. Association of methylmercury with dissolved humic acids. Environ. Sci. Technol. 36, 690–695.
Ao, M., Xu, X., Wu, Y., Zhang, C., Meng, B., Shang, L., Liang, L., Qiu, R., Wang, S., Qian, X., Zhao, L., Qiu, G., 2020. Newly deposited atmospheric mercury in a simulated rice ecosystem in an active mercury mining region: high loading, accumulation, and availability. Chemosphere 238, 124630.
Barkay, T., Gillman, M., Turner, R.R., 1997. Effects of dissolved organic carbon and salinity on bioavailability of mercury. Appl. Environ. Microbiol. 63, 4267–4271.
Beckers, F., Awad, Y.M., Beiyuan, J., Abrigata, J., Mothes, S., Tsang, D.C.W., Ok, Y.S., Rinklebe, J., 2019a. Impact of biochar on mobilization, methylation, and ethylation of mercury under dynamic redox conditions in a contaminated floodplain soil. Environ. Int. 127, 276–290.
Beckers, F., Mothes, S., Abrigata, J., Zhao, J., Gao, Y., Rinklebe, J., 2019b. Mobilization of mercury species under dynamic laboratory redox conditions in a contaminated floodplain soil as affected by biochar and sugar beet factory lime. Sci. Total Environ. 672, 604–617.
Beckers, F., Rinklebe, J., 2017. Cycling of mercury in the environment: sources, fate, and human health implications: a review. Crit. Rev. Environ. Sci. Technol. 47, 693–794.
Bergamaschi, B.A., Krabbenhoft, D.P., Aiken, G.R., Patino, E., Rumbold, D.G., Orem, W. H., 2012. Tidally driven export of dissolved organic carbon, total mercury, and methylmercury from a mangrove-dominated estuary. Environ. Sci. Technol. 46, 1371–1378.
Birdwell, J.E., Engel, A.S., 2010. Characterization of dissolved organic matter in cave and spring waters using UV–Vis absorbance and fluorescence spectroscopy. Org. Geochem. 41, 270–280.
Boening, D.W., 2000. Ecological effects, transport, and fate of mercury: a general review. Chemosphere 40, 1335–1351.
Bravo, A.G., Bouchet, S., Tolu, J., Björn, E., Mateos-Rivera, A., Bertilsson, S., 2017. Molecular composition of organic matter controls methylmercury formation in boreal lakes. Nat. Commun. 8, 14255.
Chen, Q., Jia, R., Li, L., Qu, D., 2020. Effects of high concentrations of sulfate on dissolved organic matter in paddy soils revealed by excitation-emission matrix analyzing. Chemosphere 249, 126207.
Coble, P.G., Spencer, R.G.M., Baker, A., Reynolds, D.M., 2014. Aquatic organic matter fluorescence. In: Baker, A., Reynolds, D.M., Lead, J., Coble, P.G., Spencer, R.G.M. (Eds.), Aquatic Organic Matter Fluorescence. Cambridge University Press, Cambridge, pp. 75–122.
Dittman, J.A., Shanley, J.B., Driscoll, C.T., Aiken, G.R., Chalmers, A.T., Towse, J.E., 2009. Ultraviolet absorbance as a proxy for total dissolved mercury in streams. Environ. Pollut. 157, 1953–1956.
Dong, W., Liang, L., Brooks, S., Southworth, G., Gu, B., 2010. Roles of dissolved organic matter in the speciation of mercury and methylmercury in a contaminated ecosystem in Oak Ridge, Tennessee. Environ. Chem. 7, 94–102.
Drott, A., Lambertsson, L., Björn, E., Skyllberg, U., 2008. Do potential methylation rates reflect accumulated methyl mercury in contaminated sediments? Environ. Sci. Technol. 42, 153–158.
Du, J., Liu, F., Zhao, L., Liu, C., Fu, Z., Teng, Y., 2021. Mercury horizontal spatial distribution in paddy field and accumulation of mercury in rice as well as their influencing factors in a typical mining area of Tongren City, Guizhou, China. J. Environ. Health Sci. Eng. 19, 1555–1567.
Eckley, C.S., Luxton, T.P., Stanfield, B., Baldwin, A., Holloway, J., McKernan, J., Johnson, M.G., 2021. Effect of organic matter concentration and characteristics on mercury mobilization and methylmercury production at an abandoned mine site. Environ. Pollut. 271, 116369.

Feng, X., Li, P., Qiu, G., Wang, S., Li, G., Shang, L., Meng, B., Jiang, H., Bai, W., Li, Z., Fu, X., 2008. Human exposure to methylmercury through rice intake in mercury mining areas, Guizhou province, China. Environ. Sci. Technol. 42, 326–332.
Feng, X., Qiu, G., 2008. Mercury pollution in Guizhou, southwestern China — an overview. Sci. Total Environ. 400, 227–237.
Fichot, C.G., Benner, R., 2012. The spectral slope coefficient of chromophoric dissolved organic matter (S275–295) as a tracer of terrigenous dissolved organic carbon in river-influenced ocean margins. Limnol. Oceanogr. 57, 1453–1466.
Fichot, C.G., Kaiser, K., Hooker, S.B., Amon, R.M.W., Babin, M., Bélanger, S., Walker, S. A., Benner, R., 2013. Pan-Arctic distributions of continental runoff in the Arctic Ocean. Sci. Rep. 3.
French, T.D., Houben, A.J., Desforges, J.-P.W., Kimpe, L.E., Kokelj, S.V., Poulain, A.J., Smol, J.P., Wang, X., Blais, J.M., 2014. Dissolved organic carbon thresholds affect mercury bioaccumulation in arctic lakes. Environ. Sci. Technol. 48, 3162–3168.
Frohne, T., Rinklebe, J., Langer, U., Du Laing, G., Mothes, S., Wennrich, R., 2012. Biogeochemical factors affecting mercury methylation rate in two contaminated floodplain soils. Biogeosciences 9, 493–507.
Gao, J., Liang, C., Shen, G., Lv, J., Wu, H., 2017. Spectral characteristics of dissolved organic matter in various agricultural soils throughout China. Chemosphere 176, 108–116.
Gerbig, C.A., Ryan, J.N., Aiken, G.R., 2011. The effects of dissolved organic matter on mercury biogeochemistry. In: Liu, G., Cai, Y., O'Driscoll, N. (Eds.), Environmental Chemistry and Toxicology of Mercury. John Wiley & Sons, Inc., Hoboken, New Jersey, Canada, pp. 259–292.
Graham, A.M., Aiken, G.R., Gilmour, C.C., 2013. Effect of dissolved organic matter source and character on microbial Hg methylation in Hg–S–DOM solutions. Environ. Sci. Technol. 47, 5746–5754.
Groeneveld, M., Catalán, N., Einarsdottir, K., Bravo, A.G., Kothawala, D.N., 2022. The influence of pH on dissolved organic matter fluorescence in inland waters. Anal. Methods 14, 1351–1360.
Gustave, W., Yuan, Z.-F., Sekar, R., Ren, Y.-X., Liu, J.-Y., Zhang, J., Chen, Z., 2019. Soil organic matter amount determines the behavior of iron and arsenic in paddy soil with microbial fuel cells. Chemosphere 237, 124459.
Hall, B.D., Aiken, G.R., Krabbenhoft, D.P., Marvin-DiPasquale, M., Swarzenski, C.M., 2008. Wetlands as principal zones of methylmercury production in southern Louisiana and the Gulf of Mexico region. Environ. Pollut. 154, 124–134.
Hammerschmidt, C.R., Fitzgerald, W.F., Balcom, P.H., Visscher, P.T., 2008. Organic matter and sulfide inhibit methylmercury production in sediments of New York/New Jersey Harbor. Mar. Chem. 109, 165–182.
Helms, J.R., Stubbins, A., Ritchie, J.D., Minor, E.C., Kieber, D.J., Mopper, K., 2008. Absorption spectral slopes and slope ratios as indicators of molecular weight, source, and photobleaching of chromophoric dissolved organic matter. Limnol. Oceanogr. 53, 955–969.
Hintelmann, H., Welbourn, P.M., Evans, R.D., 1995. Binding of methylmercury compounds by humic and fulvic acids. Water Air Soil Pollut. 80, 1031–1034.
Hsu-Kim, H., Kucharzyk, K.H., Zhang, T., Deshusses, M.A., 2013. Mechanisms regulating mercury bioavailability for methylating microorganisms in the aquatic environment: a critical review. Environ. Sci. Technol. 47, 2441–2456.
Hu, J., Wu, J., Qu, X., Li, J., 2018. Effects of organic wastes on structural characterizations of humic acid in semiarid soil under plastic mulched drip irrigation. Chemosphere 200, 313–321.
Huang, M., Zhou, M., Li, Z., Ding, X., Wen, J., Jin, C., Wang, L., Xiao, L., Chen, J., 2022. How do drying-wetting cycles influence availability of heavy metals in sediment? A perspective from DOM molecular composition. Water Res. 220, 118671.
Huguet, A., Vacher, L., Relexans, S., Saubusse, S., Froidefond, J.M., Parlanti, E., 2009. Properties of fluorescent dissolved organic matter in the Gironde Estuary. Org. Geochem. 40, 706–719.
Jiang, T., Bravo, A.G., Skyllberg, U., Björn, E., Wang, D., Yan, H., Green, N.W., 2018. Influence of dissolved organic matter (DOM) characteristics on dissolved mercury (Hg) species composition in sediment porewater of lakes from southwest China. Water Res. 146, 146–158.
Jiang, T., Skyllberg, U., Björn, E., Green, N.W., Tang, J., Wang, D., Gao, J., Li, C., 2017. Characteristics of dissolved organic matter (DOM) and relationship with dissolved mercury in Xiaoqing River-Laizhou Bay estuary, Bohai Sea, China. Environ. Pollut. 223, 19–30.
Jiang, T., Wang, D., Meng, B., Chi, J., Laudon, H., Liu, J., 2020. The concentrations and characteristics of dissolved organic matter in high-latitude lakes determine its ambient reducing capacity. Water Res. 169, 115217.
Kim, H., Soerensen, A.L., Hur, J., Heimbürger, L.-E., Hahm, D., Rhee, T.S., Noh, S., Han, S., 2017. Methylmercury mass budgets and distribution characteristics in the Western Pacific ocean. Environ. Sci. Technol. 51, 1186–1194.
Kuzyakov, Y., Horwath, W.R., Dorodnikov, M., Blagodatskaya, E., 2018. Chapter eight - effects of elevated CO2 in the atmosphere on soil C and N turnover. In: Horwath, W. R., Kuzyakov, Y. (Eds.), Developments in Soil Science. Elsevier, pp. 207–219.
Lambertsson, L., Nilsson, M., 2006. Organic material: the primary control on mercury methylation and ambient methyl mercury concentrations in estuarine sediments. Environ. Sci. Technol. 40, 1822–1829.
Lee, M.-H., Osburn, C.L., Shin, K.-H., Hur, J., 2018. New insight into the applicability of spectroscopic indices for dissolved organic matter (DOM) source discrimination in aquatic systems affected by biogeochemical processes. Water Res. 147, 164–176.
Lescord, G.L., Emilson, E.J.S., Johnston, T.A., Branfireun, B.A., Gunn, J.M., 2018. Optical properties of dissolved organic matter and their relation to mercury concentrations in water and biota across a remote freshwater drainage basin. Environ. Sci. Technol. 52, 3344–3353.
Li, H., Yang, Y., Si, Y., Liu, Z., 2017. Effects of short-term global warming and precipitation reduction on the quantity and spectral characteristics of soil DOM in Cunninghamia lanceolata plantation. Chin. J. Eco-Agric. 25, 949–957.
Li, X.-M., Sun, G.-X., Chen, S.-C., Fang, Z., Yuan, H.-Y., Shi, Q., Zhu, Y.-G., 2018. Molecular chemodiversity of dissolved organic matter in paddy soils. Environ. Sci. Technol. 52, 963–971.
Liang, L., Horvat, M., Cernichiari, E., Gelein, B., Balogh, S., 1996. Simple solvent extraction technique for elimination of matrix interferences in the determination of methylmercury in environmental and biological samples by ethylation-gas chromatography-cold vapor atomic fluorescence spectrometry. Talanta 43, 1883–1888.
Lin, H., Morrell-Falvey, J.L., Rao, B., Liang, L., Gu, B., 2014. Coupled mercury–cell sorption, reduction, and oxidation on methylmercury production by geobacter sulfurreducens PCA. Environ. Sci. Technol. 48, 11969–11976.
Liu, J., Liang, J., Bravo, A.G., Wei, S., Yang, C., Wang, D., Jiang, T., 2021. Anaerobic and aerobic biodegradation of soil-extracted dissolved organic matter from the water-level-fluctuation zone of the Three Gorges Reservoir region, China. Sci. Total Environ. 764, 142857.
Liu, J., Lu, B., Poulain, A.J., Zhang, R., Zhang, T., Feng, X., Meng, B., 2022a. The underappreciated role of natural organic matter bond Hg(II) and nanoparticulate HgS as substrates for methylation in paddy soils across a Hg concentration gradient. Environ. Pollut. 292, 118321.
Liu, J., Wang, D., Zhang, J., Liem-Nguyen, V., Huang, R., Jiang, T., 2020. Evaluation of Hg methylation in the water-level-fluctuation zone of the Three Gorges Reservoir region by using the MeHg/HgT ratio. Ecotoxicol. Environ. Saf. 195, 110468.
Liu, J., Zhao, L., Kong, K., Abdelhafiz, M.A., Tian, S., Jiang, T., Meng, B., Feng, X., 2022b. Uncovering geochemical fractionation of the newly deposited Hg in paddy soil using a stable isotope tracer. J. Hazard Mater. 433, 128752.
Liu, Y.R., Yu, R.Q., Zheng, Y.M., He, J.Z., 2014. Analysis of the microbial community structure by monitoring an Hg methylation gene (hgcA) in paddy soils along an Hg gradient. Appl. Environ. Microbiol. 80, 2874–2879.
Luo, H., Cheng, Q., He, D., Zeng, G., Sun, J., Li, J., Pan, X., 2022. Binding of methylmercury to humic acids (HA): influence of solar radiation and sulfide addition reaction of HA. Sci. Total Environ. 827, 154356.
Mazrui, N.M., Jonsson, S., Thota, S., Zhao, J., Mason, R.P., 2016. Enhanced availability of mercury bound to dissolved organic matter for methylation in marine sediments. Geochem. Cosmochim. Acta 194, 153–162.
McKnight, D.M., Boyer, E.W., Westerhoff, P.K., Doran, P.T., Kulbe, T., Andersen, D.T., 2001. Spectrofluorometric characterization of dissolved organic matter for indication of precursor organic material and aromaticity. Limnol. Oceanogr. 46, 38–48.
Meng, B., Feng, X., Qiu, G., Cai, Y., Wang, D., Li, P., Shang, L., Sommar, J., 2010. Distribution patterns of inorganic mercury and methylmercury in tissues of rice (Oryza sativa L.) plants and possible bioaccumulation pathways. J. Agric. Food Chem. 58, 4951–4958.
Meng, B., Feng, X., Qiu, G., Liang, P., Li, P., Chen, C., Shang, L., 2011. The process of methylmercury accumulation in rice (Oryza sativa L.). Environ. Sci. Technol. 45, 2711–2717.
Mostofa, K.M.G., Liu, C.-q., Yoshioka, T., Vione, D., Zhang, Y., Sakugawa, H., 2013. Fluorescent dissolved organic matter in natural waters. In: Mostofa, K.M.G., Yoshioka, T., Mottaleb, A., Vione, D. (Eds.), Photobiogeochemistry of Organic Matter: Principles and Practices in Water Environments. Springer Berlin Heidelberg, Berlin, Heidelberg, pp. 429–559.
Nayak, A.K., Rahman, M.M., Naidu, R., Dhal, B., Swain, C.K., Nayak, A.D., Tripathi, R., Shahid, M., Islam, M.R., Pathak, H., 2019. Current and emerging methodologies for estimating carbon sequestration in agricultural soils: a review. Sci. Total Environ. 665, 890–912.
Nowicki, S., Lapworth, D.J., Ward, J.S.T., Thomson, P., Charles, K., 2019. Tryptophan-like fluorescence as a measure of microbial contamination risk in groundwater. Sci. Total Environ. 646, 782–791.
Ohno, T., 2002. Fluorescence inner-filtering correction for determining the humification index of dissolved organic matter. Environ. Sci. Technol. 36, 742–746.
Ortega, S.H., Catalán, N., Björn, E., Gröntoft, H., Hilmarsson, T.G., Bertilsson, S., Wu, P., Bishop, K., Levanoni, O., Bravo, A.G., 2018. High methylmercury formation in ponds fueled by fresh humic and algal derived organic matter. Limnol. Oceanogr. 63, S44–S53.
Paranjape, A.R., Hall, B.D., 2017. Recent advances in the study of mercury methylation in aquatic systems. FACETS 2, 85–119.
Praise, S., Ito, H., Sakuraba, T., Pham, D.V., Watanabe, T., 2020. Water extractable organic matter and iron in relation to land use and seasonal changes. Sci. Total Environ. 707, 136070.
Pu, Q., Zhang, K., Poulain, A.J., Liu, J., Zhang, R., Abdelhafiz, M.A., Meng, B., Feng, X., 2022. Mercury drives microbial community assembly and ecosystem multifunctionality across a Hg contamination gradient in rice paddies. J. Hazard Mater. 435, 129055.
Qin, X.-q., Yao, B., Jin, L., Zheng, X.-z., Ma, J., Benedetti, M.F., Li, Y., Ren, Z.-l., 2020. Characterizing soil dissolved organic matter in typical soils from China using fluorescence EEM–PARAFAC and UV–visible absorption. Aquat. Geochem. 26, 71–88.
Qiu, G., Feng, X., Li, P., Wang, S., Li, G., Shang, L., Fu, X., 2008. Methylmercury accumulation in rice (Oryza sativa L.) grown at abandoned mercury mines in Guizhou, China. J. Agric. Food Chem. 56, 2465–2468.
Qiu, G., Feng, X., Meng, B., Wang, X., 2011. Methylmercury in rice (Oryza sativa L.) grown from the Xunyang Hg mining area, Shaanxi province, northwestern China. Pure Appl. Chem. 84, 281–289.

Ravichandran, M., 2004. Interactions between mercury and dissolved organic matter—a review. Chemosphere 55, 319–331.
Schartup, A.T., Mason, R.P., Balcom, P.H., Hollweg, T.A., Chen, C.Y., 2013. Methylmercury production in estuarine sediments: role of organic matter. Environ. Sci. Technol. 47, 695–700.
Shang, P., Lu, Y., Du, Y., Jaffé, R., Findlay, R.H., Wynn, A., 2018. Climatic and watershed controls of dissolved organic matter variation in streams across a gradient of agricultural land use. Sci. Total Environ. 612, 1442–1453.
Spencer, R.G.M., Butler, K.D., Aiken, G.R., 2012. Dissolved organic carbon and chromophoric dissolved organic matter properties of rivers in the USA. J. Geophys. Res.: Biogeosciences 117.
Tong, H., Simpson, A.J., Paul, E.A., Simpson, M.J., 2021. Land-Use change and environmental properties alter the quantity and molecular composition of soil-derived dissolved organic matter. ACS Earth Space Chem. 5, 1395–1406.
Ullrich, S.M., Tanton, T.W., Abdrashitova, S.A., 2001. Mercury in the aquatic environment: a review of factors affecting methylation. Crit. Rev. Environ. Sci. Technol. 31, 241–293.
USEPA, 2001. Method 1630 Methylmercury in Water by Distillation, Aqueous Ethylation, Purge and Trap, and Cold Vapor Atomic Fluorescence Spectrometry CVAFS. United States Environmental Protection Agency, Washington, DC (EPA-821-R-01-020).
USEPA, 2002. Method 1631, Revision E: Mercury in Water by Oxidation, Purge and Trap, and Cold Vapor Atomic Fluorescence Spectrometry. US Environmental Protection Agency Washington, DC.
USEPA, 2017. Methylmercury in Water, Distillation, Aqueous Ethylation, Purge & Trap, GC-Pyrolysis-CVAFS. (Based on Method 1630). United States Environmental Protection Agency.
Wang, J., Shaheen, S.M., Jing, M., Anderson, C.W.N., Swertz, A.-C., Wang, S.-L., Feng, X., Rinklebe, J., 2021. Mobilization, methylation, and demethylation of mercury in a paddy soil under systematic redox changes. Environ. Sci. Technol. 55, 10133–10141.
Wang, Y., Liu, J., Liem-Nguyen, V., Tian, S., Zhang, S., Wang, D., Jiang, T., 2022a. Binding strength of mercury (II) to different dissolved organic matter: the roles of DOM properties and sources. Sci. Total Environ. 807, 150979.
Wang, Z., Cao, J., Meng, F., 2015. Interactions between protein-like and humic-like components in dissolved organic matter revealed by fluorescence quenching. Water Res. 68, 404–413.
Wang, Z., Han, R., Muhammad, A., Guan, D.-X., Zama, E., Li, G., 2022b. Correlative distribution of DOM and heavy metals in the soils of the Zhangxi watershed in Ningbo city, East of China. Environ. Pollut. 299, 118811.
Watras, C.J., Back, R.C., Halvorsen, S., Hudson, R.J.M., Morrison, K.A., Wente, S.P., 1998. Bioaccumulation of mercury in pelagic freshwater food webs. Sci. Total Environ. 219, 183–208.
Weishaar, J.L., Aiken, G.R., Bergamaschi, B.A., Fram, M.S., Fujii, R., Mopper, K., 2003. Evaluation of specific ultraviolet absorbance as an indicator of the chemical composition and reactivity of dissolved organic carbon. Environ. Sci. Technol. 37, 4702–4708.
Wu, H., Ding, Z., Liu, Y., Liu, J., Yan, H., Pan, J., Li, L., Lin, H., Lin, G., Lu, H., 2011. Methylmercury and sulfate-reducing bacteria in mangrove sediments from Jiulong River Estuary, China. J. Environ. Sci. 23, 14–21.
Yang, L., Hur, J., 2014. Critical evaluation of spectroscopic indices for organic matter source tracing via end member mixing analysis based on two contrasting sources. Water Res. 59, 80–89.
Yang, Y.-k., Zhang, C., Shi, X.-j., Lin, T., Wang, D.-y., 2007. Effect of organic matter and pH on mercury release from soils. J. Environ. Sci. 19, 1349–1354.
Yuan, S., Peng, S., 2022. Food-energy-emission nexus of rice production in China. Crop Environ. 1, 59–67.
Zhang, H., Feng, X., Larssen, T., Qiu, G., Vogt, R.D., 2010. In inland China, rice, rather than fish, is the major pathway for methylmercury exposure. Environ. Health Perspect. 118, 1183–1188.
Zhang, S., Wang, M., Liu, J., Tian, S., Yang, X., Xiao, G., Xu, G., Jiang, T., Wang, D., 2022. Biochar affects methylmercury production and bioaccumulation in paddy soils: insights from soil-derived dissolved organic matter. J. Environ. Sci. 119, 68–77.
Zhang, Y.L., Qin, B.Q., Chen, W.M., Zhu, G.W., 2005. A preliminary study of chromophoric dissolved organic matter (CDOM) in lake taihu, a shallow subtropical lake in China. Acta Hydrochim. Hydrobiol. 33, 315–323.
Zhao, L., Anderson, C.W.N., Qiu, G., Meng, B., Wang, D., Feng, X., 2016a. Mercury methylation in paddy soil: source and distribution of mercury species at a Hg mining area, Guizhou Province, China. Biogeosciences 13, 2429–2440.
Zhao, L., Qiu, G., Anderson, C.W.N., Meng, B., Wang, D., Shang, L., Yan, H., Feng, X., 2016b. Mercury methylation in rice paddies and its possible controlling factors in the Hg mining area, Guizhou province, Southwest China. Environ. Pollut. 215, 1–9.